A NEW APPROACH TO ANTI-FORGERY USING SALIENCY GUIDED IMAGE WATERMARKING

QUANG HUY PHAM, NAM ANH DAO*

Electric Power University,
235 Hoang Quoc Viet Street, Bac Tu Liem District, Ha Noi, Viet Nam

Crossref
Similarity Check
Powered by iThenticate

Abstract. Using various image characteristics as a secret key, the cryptanalytic watermarking method is known for enhancing the resilience of authentication systems and protecting against forgery attempts when concealing information within a host image. This study introduces a new approach that leverages saliency features to establish a secret key, subsequently utilizing this key as a parameter for embedding and extracting watermarks. Despite the alteration of image features during watermark embedding, we suggest employing learning techniques in conjunction with saliency models to ensure the robustness of watermark extraction. The proposed image watermarking technique incorporates SVM learning and multiple saliency models. Our findings demonstrate the effectiveness of the cryptanalytic watermarking method in maintaining the watermark's invisibility and stability. The benefits of the saliency feature-based approach for anti-forgery are evident through experiments conducted on a standard dataset.

Keywords. Image watermarking, anti-forgery, saliency, learning.

1. INTRODUCTION

Watermarking is a key aspect of multimedia technologies, serving various purposes including authentication and anti-forgery measures. The process of digital watermarking typically involves four main steps: embedding, distribution, attack, and extraction, with the attack phase focusing on potential content alterations [6]. It is crucial to ensure robustness, which involves maintaining the similarity between the extracted watermark and the original watermark. Watermarks are designed to be either invisible or visible. Invisible watermarking is often used for ownership protection, as embedding a hidden watermark in an image can help deter piracy. Conversely, visible watermarking is more suitable for drawing attention to textual copyrights. Significant attention has been given to enhancing watermarked images by strategically placing the watermark in well-hidden areas of the image.

As sub-regions that attract high visibility are considered crucial components of images [11], they are typically retained and not removed during image alterations. Therefore, it is logical to embed watermarks visibly in these salient sub-regions to draw attention to textual copyrights. Additionally, image areas with low visibility are ideal for embedding imperceptible watermarks. This approach aligns with steganography, facilitating covert

*Corresponding author.

E-mail addresses: huypq@epu.edu.vn (Q.H. Pham); anhdn@epu.edu.vn (N.A Dao).

communication. In the context of invisible saliency-based watermarking, if the encryption technique used does not degrade image quality and ensures that the area containing the embedded mark remains non-salient, the watermark should remain undetectable. It is a challenge because the encryption process will alter the image.

The wide range of saliency models used to identify salient regions necessitates that any steganalysis method based on saliency must incorporate multiple models to ensure the robustness of extracted watermarks. The main contributions of the paper are as follows: using saliency features to generate a secret key, which is then used as a parameter for extracting and embedding watermarks. Additionally, this paper introduces saliency feature learning, which outlines the process of generating a secret key from saliency features to enhance the robustness of watermark extraction, thereby significantly enhancing its efficacy.

The structure of the paper is organized as follows. Section 1 introduces watermarking and its applications. In Section 2, we review related works such as some digital watermarking works. In Section 3, we present the proposed method using SVM learning and the assistance of several saliency models. The discussions and evaluations of the results are presented in Section 4. Finally, some concluding remarks were made in Section 5.

2. RELATED WORK

As previously mentioned, the visual attention approach is akin to image feature extraction but places greater emphasis on visual appeal and the interpretation of regions with the highest visual interest. This technique involves segmenting regions of visual interest, which is beneficial when determining if a specific area of the host image is suitable for watermark embedding without compromising perceived visual quality.

Recent studies have further explored the application of saliency features in image watermarking. For instance, Wang et al [19] proposed the DARI-Mark framework, which integrates deep learning and attention networks for robust image watermarking, demonstrating significant resilience against various attacks such as JPEG compression and noise addition. Similarly, Ge et al. [10] introduced a deep neural network-based scheme for robust document image watermarking, highlighting the efficacy of deep learning in this domain. Panchikkil et al. [18] explored an ensemble learning approach for reversible data hiding, expanding the scope of watermarking techniques in encrypted images. Ros [8] discussed the latest developments and applications of image watermarking, including the integration of cryptography and deep learning approaches.

These studies present various strengths and weaknesses. Wang et al.'s method excels in robustness and imperceptibility, leveraging the attention mechanism to enhance watermark embedding and extraction. However, its complexity may increase computational costs. Ge et al.'s approach demonstrates strong performance in document image watermarking but may require further validation in diverse application scenarios. Panchikkil et al.'s reversible data hiding technique offers high security and robustness, yet its effectiveness in dynamic environments needs further exploration. Ros's comprehensive review provides a solid foundation for understanding current trends but highlights the ongoing challenges in achieving a balance between robustness, capacity, and imperceptibility.

By analyzing these strengths and weaknesses, the proposed method can be better contextualized, showcasing its unique contributions and addressing identified gaps in the existing

literature.

Several principles govern the estimation of visual attention. One method involves assessing saliency detection based on the local data structure of the image [4], where the similarity of features at a pixel to its neighboring pixels is evaluated. In another study [14], the sparse foreground location is approximated on a sparse background using Discrete Cosine Transform (DCT). Other research focuses on utilizing local contrast and global rarity measures for feature extraction [24]. This involves describing contrasts against randomly selected neighboring and peripheral regions, thereby differentiating between targets and distractors in saliency assessment [2].

Next, we will explore some research on digital watermarking techniques, specifically those based on visual attention, which are relevant to the proposed approach. These works involve using a saliency level to identify visually salient and non-salient areas in an image. To maintain visual quality, stronger watermarks are inserted into visually salient areas and weaker ones into non-salient areas [20]. While previous methods used wavelets for this purpose, our approach introduces saliency learning to choose the embedding regions, ensuring minimal impact on visual quality. The watermarking field also investigates steganographic techniques like LSB matching [13], where the decision to embed or extract a watermark bit at a pixel is random. Some approaches modify the LSB method to minimize changes in the host image, while others prioritize near-optimal solutions. Unlike traditional LSB implementations [7], our method leverages saliency to guide the watermark embedding process in changing the host image. By using saliency values, we determine where to embed or extract the watermark at a pixel level [15]. The proposed technique incorporates saliency to focus on regions of interest, embedding a robust watermark in DCT coefficients of these regions and a fragile watermark in low sub-bands [3]. This method allows for the application of various saliency models to estimate saliency, ensuring minimal changes in subregions when watermarking is applied.

3. METHOD

The algorithm described here, known as the Saliency Guided Image Watermarking (SGW), is designed for anti-forgery purposes [1]. The watermark used in this algorithm is typically fragile and aimed at protecting the data. Similar to a previous study [12], mathematical concepts are employed to articulate the watermarking process. The process of embedding information can be likened to encoding in a cryptographic context and is defined by function (1) which links the host image u, watermark w, and key k to the resulting embedded or encoded image v. It should be noted that the key k may not always be utilized in this process. The extraction of information, analogous to decoding in cryptography, is outlined by function (2)

$$v = \text{encode}(u, w, \langle k \rangle), \tag{1}$$

$$w = \text{decode}(v, \langle u \rangle, \langle k \rangle). \tag{2}$$

3.1. Feature detectors

Several saliency models are available that can function as feature detectors for the host image, and the key k can be derived from these features. This allows the encoding functions

(1) to incorporate a hidden key, and the decoding functions (2) can deduce the key from the input list (3). Additionally, only the encoded image v is utilized in the decoding process (4). The ultimate blind anti-forgery verification is carried out by function (5), which outputs a yes or no response depending on whether the watermark w is present in the image v

$$v = \text{encode}(u, w), \tag{3}$$

$$w = \text{decode}(v), \tag{4}$$

$$b = \text{detect}(v, w), \ b \in \{0, 1\}. \tag{5}$$

This technique employs a multi-subregion strategy, as the domain space of the host image inherently resembles a 2D Cartesian plane, offering numerous possibilities to divide the space into subregions ri for watermark insertion. Consequently, for each image in the training set L, saliency features can be computed for its respective subregions. This facilitates the creation of a saliency feature matrix f, as described in equation (6)

$$f_i^j = \text{saliency}(u(r_i^j)), \ i = 1, n, \ j \in L. \tag{6}$$

When dividing the image space into subregions to conceal a watermark, it is crucial to carefully select the subregion locations. For watermarking aimed at anti-forgery purposes, the subregions should be positioned near the image borders where low saliency is typically observed. A basic configuration involves four small rectangles ($n = 4$) aligned with the edges of the image. By encoding the watermark in different subregions r_i, the objective is to pinpoint a subregion where the insertion of the watermark minimally alters the saliency feature. By applying a saliency model to each region before and after encoding, the degree of change can be evaluated as indicated in equation (7). Subsequently, the subregion that exhibits the smallest variation is identified by specifying its index (8)

$$d_i^j = \left\| \text{saliency}(u(r_i^j)) - \text{saliency}(v(r_i^j)) \right\|_p, \ i = 1, n, \tag{7}$$

$$i_*^j = \arg\min_i d_i^j. \tag{8}$$

3.2. The proposed model

Having designated the region index (8) as a class, we now focus on training the dataset from equation (6) to generate the kernel K. Various learning methods can be utilized for this task, and in our methodology, we opt for the Support Vector Machine (SVM) [15] due to its ability to efficiently conduct non-linear classification by implicitly mapping inputs into high-dimensional feature spaces (9)

$$K = \text{training}(f_i^j|_{i=1:n}, i_*^j), \ j \in L. \tag{9}$$

During the testing phase, we have a data matrix f (10) comprising rows that contain the saliency features of subregions from test images T. The learned kernel K enables us to identify a subregion where the saliency features can be altered minimally through watermark embedding (11). The index of the subregion serves as a secret key for watermarking in both the encoding and decoding phases

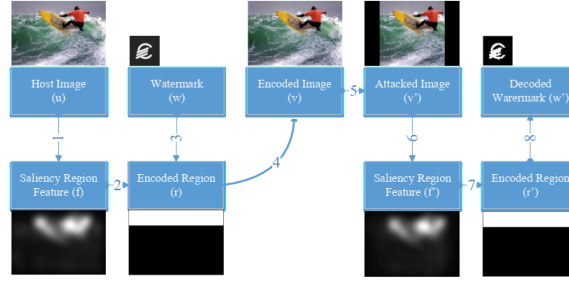$$f_i^k = \text{saliency}(u(r_i)), \ i = 1, n, \ k \in T, \tag{10}$$

Figure 1: Process of watermarking with the saliency features by SGW algorithm

$$i_*^j = \text{test}(f_i^j|_{i=1:n}, K), \ j \in T. \tag{11}$$

The feature matrix relies on a saliency model that estimates visual attention in the host image space (6). In this context, we employ four saliency detection methods. The first model assesses the saliency by measuring the resemblance of a pixel x to its surroundings y using the Self-Resemblance (SR) measure [23] as defined in equation (12). It is important to note that the Cosine similarity metric is employed for calculating the self-resemblance

$$\text{saliency}^{SR}(u(x)) = \frac{1}{\sum\limits_{y} \exp\left(\frac{-1+d_{\text{cosine}}(u(x),u(y))}{\sigma^2}\right)}. \tag{12}$$

When employing Sparse Signal Mixing (SSM), saliency is determined based on the spatial positioning of a sparse foreground concealed within a spectrally sparse background [9], as outlined in equations (13-14). This method operates under the assumption that the image background has sparse support in the Discrete Cosine Transform (DCT) basis, and g represents a Gaussian kernel

$$\ddot{u} = \text{iDCT}(\text{sign}(\text{DCT}(u))), \tag{13}$$

$$\text{saliency}^{SSM}(x) = g * (\ddot{u} \circ \ddot{u}). \tag{14}$$

A detailed examination revealed that comparing low-level luminance and chrominance attributes leads to the identification of medium-level features such as image orientations [21]. Subsequently, cross-scale rarity quantization is conducted on the probability of pixel occurrences to estimate saliency, with the premise that locally contrasting and globally uncommon features convey saliency (15)

$$\text{saliency}^{RARE}(x) = -\log\left(\frac{1}{c\|u(x)\|}\sum_{k=1}^{c} o_k\right), \tag{15}$$

where, c is the scale, o_k is the occurrence value of the current pixel $u(x)$ within the k_{th} scale.

Building on the effectiveness of principal component analysis (PCA) [17], visual saliency assessment is achieved using PCA to differentiate between visual targets and distractors [8]. In this approach, projecting images onto different subspaces enables the assessment of average contrasts between randomly chosen neighbors for each image patch. Subsequently, a learning process for subspace selection and integration results in the identification of an optimized

weighting solution (16) and the estimation of saliency (17), where ϕ represents Random Contrasts (RC) for a patch and K denotes the image training set, with T and D representing the sets of targets and distractors for images u

$$w^* = \min_{w} \sum_{K} \sum_{T} \sum_{D} \exp\left(w^T \phi(D) - w^T \phi(T)\right), \tag{16}$$

$$\text{saliency}^{RC}(x) = w^* \phi(u). \tag{17}$$

To simplify the complexity of steganography operations, we employ the Arnold Transformation algorithm [16] for the initial encoding of the watermark (18). Subsequently, following the concept of Least Significant Bit (LSB), the watermark is combined with the blue channel of region r_i* guided by the saliency feature f (19)

$$w_A = \text{Arnold}(w), \tag{18}$$

$$v = \text{mixing}_{LSB}(w_A, u(r_i*), f(r_i*)). \tag{19}$$

The decoding process commences by identifying a watermark w_A within the encrypted region of the blue channel in image v through LSB manipulation guided by saliency (20). Finally, the watermark w is extracted from w_A using the inverse Arnold transform

$$w_A = \text{detect}_{LSB}(v(r_i*), f(r_i*)), \tag{20}$$

$$w = \text{iArnold}(w_A). \tag{21}$$

We investigate how image features obtained from various saliency models (12-17), regardless of their method of estimation-such as SR [19], SSM [10], RARE [18], and RC [8]-can be utilized for watermark encoding and decoding tasks (3-11). Figure 1 outlines the watermarking procedure using an example host image u. After estimating the saliency of the image, the saliency feature f is determined for each subregion. The SVM kernel aids in selecting a subregion r within the top portion of the image. As the watermark w is embedded, the modified host image v differs slightly from its original form, and may be prone to attacks like cropping. Subsequently, upon discovering the saliency feature f' for the modified image v', the SVM kernel identifies the subregion r' where the watermark w' has been embedded, enabling the decoding of the watermark.

4.   RESULTS AND DISCUSSION

4.1.   Examples of results

This section delves into the robustness of the described method in conjunction with specific saliency models. The efficacy of the method was evaluated using the MSRA10K Salient Object Database [5], which comprises 10,000 real images. The database was randomly divided into training and test sets. Through experiments involving four saliency models, we assessed performance by leveraging SVM-generated kernels. Additionally, various attack types were employed during the testing phase, including scaling, rotation, additive Gaussian noise, salt and pepper noise, histogram equalization, median filter, and cropping.

Figure 2 illustrates an instance of embedding a black and white logo into an image titled 112691.jpg from MSRA10K, utilizing the SR [19], SSM [10], RARE [18], and RC [8]
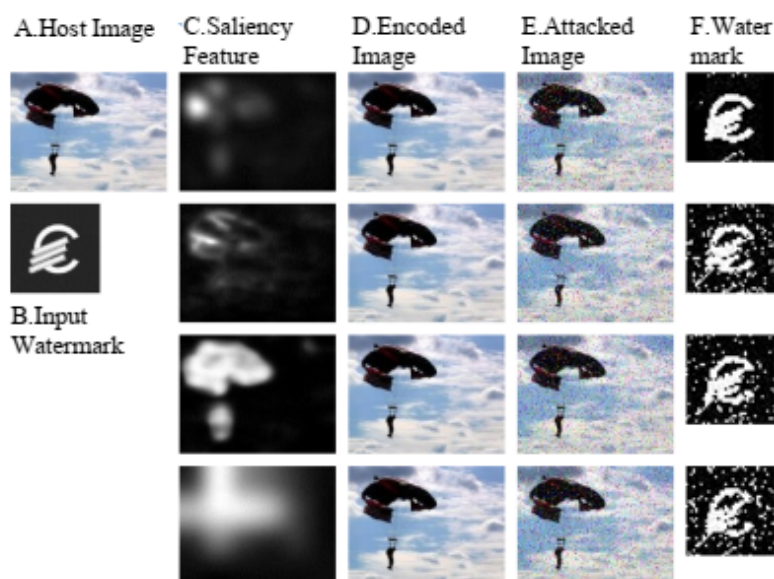
Figure 2: Embedding a black-white logo to image 112691.jpg from MSRA10K, applying four saliency models: SR [19] in the 1st row, SSM [10] - 2nd row, RARE [18] - 3rd row and RC [8] - 4th row.

saliency models (Figure 2C). As anticipated, the addition of Gaussian noise during the attack phase resulted in a noisy appearance of the encoded host image (Figure 2E). The decoded watermarks from the four scenarios exhibited varying levels of degradation due to the noise attack and the influence of saliency features (Figure 2F). The figure also displays an example of attacks, where a host image (A) and watermark (B) lead to the creation of an encoded image (D) with the assistance of saliency features (C).

Subsequently, the image undergoes various attacks, including rotation by 90° and -90° (F), additive Gaussian noise (F), salt and pepper noise (G), application of a median filter (H), and cropping by 90% (I). The extracted watermarks from the attacked images exhibit varying levels of degradation (J). It is evident that the degradation caused by a 90° rotation is minimal (F), whereas the application of a median filter results in significant degradation. The remaining attacks also induce noticeable degradation, albeit preserving the majority of the watermark.

We have thus far examined pairwise comparisons between host images and encoded images, assessing the invisibility of the watermark using metrics such as precision, recall, F-measure [18], sum of absolute differences (SAD) [17], structural similarity (SSIM) [5], mean squared error (MSE) [22], and PSNR [16]. As the decoded watermarks are impacted by various attacks, they are matched against the original versions to underscore the fragility of the watermark. To evaluate the effectiveness of the watermarking process, the following metrics are used:

- SAD (Sum of Absolute Differences): This metric calculates the absolute difference between the pixels of the original and watermarked images, providing a measure of the total variation.

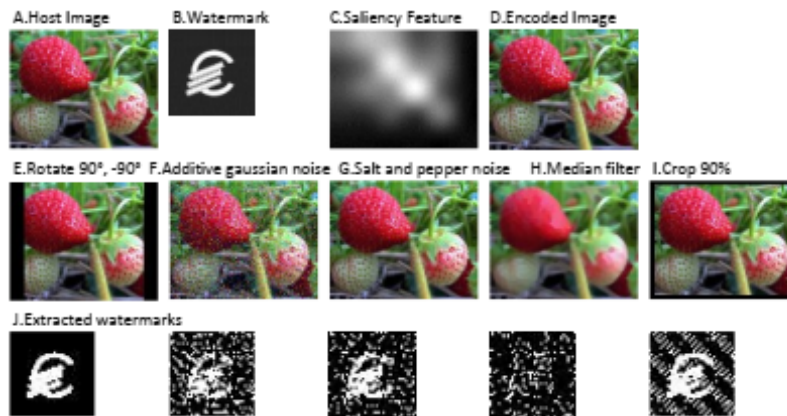- MSE (Mean Squared Error): A common metric for image quality assessment that

Figure 3: Embedding a black white logo to image 112691.jpg from MSRA10K, applying four saliency models: SR [19] in the 1st row, SSM [10] - 2nd row, RARE [18] - 3rd row and RC [8] - 4th row.

computes the average squared difference between the original and watermarked images.

- F-measure: This metric combines precision and recall to provide a single score, often used to evaluate the accuracy of watermark detection.

- SSIM (Structural Similarity Index): Measures the similarity between two images based on luminance, contrast, and structure, providing a perception-based quality assessment.

- PSNR (Peak Signal-to-Noise Ratio): This metric measures the ratio between the maximum possible power of a signal and the power of corrupting noise, expressed in decibels.

- Precision: The ratio of correctly identified watermark bits to the total number of bits identified, indicating the accuracy of watermark detection.

These metrics are essential for assessing the invisibility and stability of the watermark, ensuring that the watermarking process maintains image quality while providing robust protection.

4.2. Evaluations and discussions

Figure 4 presents the average metrics for the invisibility of the watermark for each saliency model: 4 saliency models exhibit high levels of invisibility. This underscores the benefit of the proposed saliency-based approach, attributed to the selection of non-salient regions for concealing the watermark and the minimal impact of embedding information on saliency features. The degradation of the watermark observed is a result of the watermark embedding process itself: the saliency feature changes after encoding, and during blind decoding, the saliency feature of the encoded image is used to extract the watermark.

The choice of saliency features for salient and non-salient regions is based on their visibility and impact on image quality. Embedding watermarks in salient regions ensures they are noticeable, which is useful for copyright protection. Conversely, embedding in non-salient regions maintains image quality and keeps the watermark hidden, aligning with steganography principles. Comparing the two, salient region watermarking is more suited for visible watermarks where detection is necessary, while non-salient region watermarking is ideal for invisible watermarks, preserving the image's original appearance.
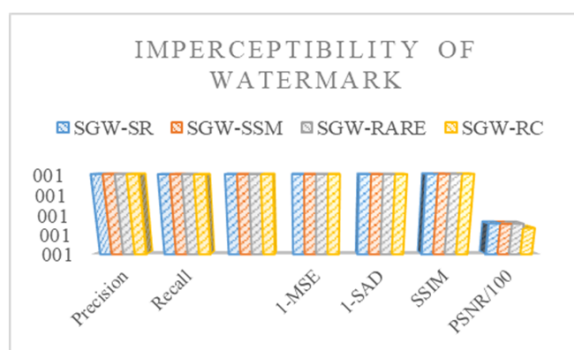
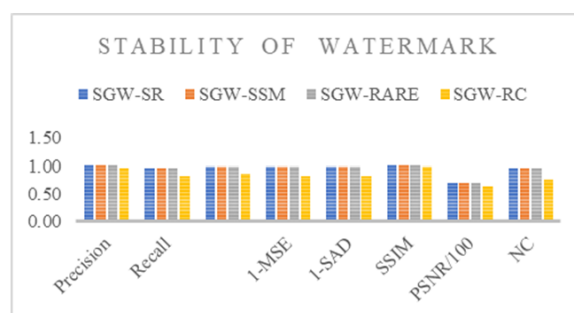Figure 4: Imperceptibility of watermark

Figure 5: Stability of watermark

To evaluate the stability of the watermark, the comparison between the original watermark and the extracted watermark can be assessed using quality metrics such as SAD, MSE, F-measure, SSIM, PSNR, precision,... [6]. Figure 5 shows the quality of the encoding process for the four saliency models. The approach utilizing the saliency models SR [19], SSM [10], RARE [18] achieved the highest scores in Precision, PSNR, and NC. The RC [8] method outperformed in MSE and SSIM metrics.

In Figure 6, it is evident that the proposed method exhibits resilience against 90° and -90° rotation attacks, but vulnerability to attacks such as histogram equalization and 45° and -45° rotation. Moreover, the PSNR results of other methods face similar attack types, albeit originating from a distinct dataset. Specifically, the ROI [20] method is tested on three host images and one watermark, while LSB [2] is evaluated on four images.

The experiments involved constructing kernels for each saliency model and individual subregions, highlighting the robustness of saliency through the creation of kernel machines. Figure 6 presents examples of the kernels from learning linkage of rare saliency features RARE [24] and the selection of the top subregion for watermark. The SVM training was carried out in a domain space of 4 dimensions which correspond to 4 sub regions in the saliency feature vector (5). For illustration by a map in 2D space, we present the relationship of each pair of sub-regions with the selection decision for the top sub-region.

Figure 7a displays the area in the percentage of the top sub-region by the horizontal axis and the area in the percentage of the bottom sub-region by the vertical axis. Dots with blue marks are samples for class "go" meaning the process for a selection of the top sub-
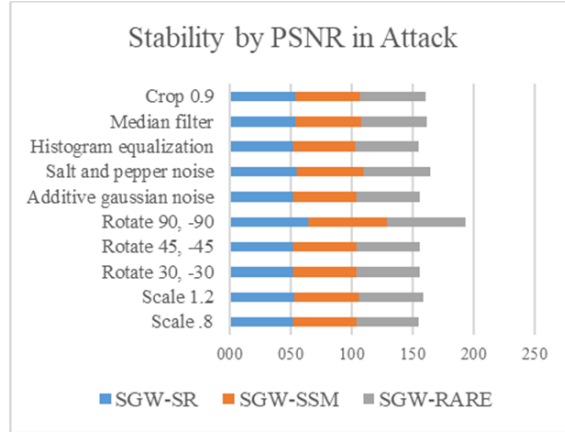
Figure 6: Stability of watermark again attacks

region with the expectation of an unremarkable change of saliency feature for this sub-region after embedding the watermark. Dots in yellow marks are samples for class "no-go" for the expectation of a remarkable change of saliency feature.

The black border represents the kernel obtained through training and delineates the classification space. This border aids in deciding which sub-region to choose for watermarking. The relationship between the top and left sub-regions regarding classification is depicted in Figure 7b, showing other samples and the border. A similar relationship is shown for the top and right sub-regions in Figure 7f. In Figure 7d, the blue color occupies most of the decision space for "go", while only a small space in Figure 7c is masked by the color. At least three rounded sub-regions in Figure 7e are designated for the decision "go".

This detailed analysis helps understand the selection of sub-regions for embedding watermarks based on their classification. The black border, derived from training, illustrates how the classification space is divided, facilitating the selection of appropriate sub-regions. By analyzing the relationship of these sub-regions to classification, as seen in Figure 7b, 7c, 7d, 7e, and 7f, we can determine the best areas for embedding the watermark. The use of blue and yellow dots in the figures indicates regions where embedding the watermark will either minimally affect the saliency feature ("go") or significantly affect it ("no-go"), guiding the watermark embedding process effectively.

4.3. Computational complexity

So far we have presented our watermarking method by learning non-saliency with demonstrated robustness for two associated saliency models. Since the selection of a proper sub-region is conducted by searching in a set of predefined sub-regions, the computational complexity of the method is proportional to the number of sub-regions.

Compute the saliency map S for the entire image I and divide it into sub-regions r_i. Extract saliency features for each sub-region and create a feature matrix f. Use the training set L to generate the kernel K using a Support Vector Machine (SVM). Identify the subregion with minimal saliency feature alteration and embed the watermark W using the key kkk. For test images T, apply the kernel K to identify subregions for watermark embedding and
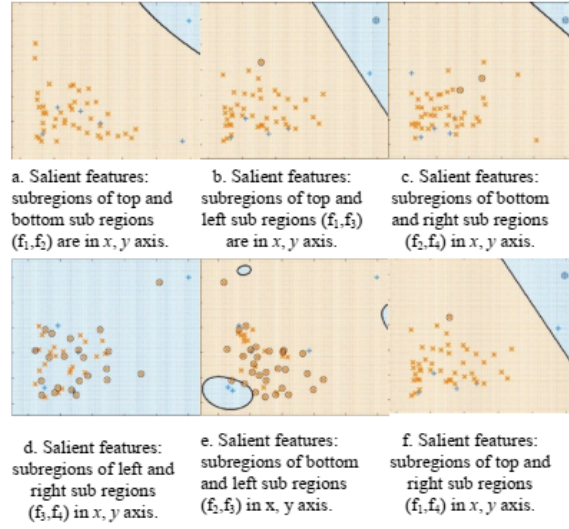
Figure 7: Learning kernels used for selection sub-region by saliency features. Dots with blue marks are samples for class "go" selection in the top sub-region with the expectation of an unremarkable change of saliency feature for this sub-region after embedding a watermark. Dots in yellow marks are samples for class "no-go" for the expectation of a remarkable change of saliency after embedding the watermark.

ensure minimal impact on saliency features. During decoding, use the key k to extract the watermark from the identified subregion.

The computational performance of our method significantly depends on estimating the computational efforts O, $O = O_s + O_w$, where O_s and O_w represent the computational complexity of the saliency model and the message embedding method, respectively. Let m denote the size of the image and n represent the size of the subregion. It is important to note that saliency detection is conducted on the entire image, whereas message embedding is carried out solely on the subregion.

Considering the descriptions of self-resemblance [19], sparse saliency [10], rare saliency [18], and random contrasts [8] for image embedding, these methods all exhibit linear complexity. With the size of the input image denoted as $O_f = O(m)$ and $O_w = O(n)$, where $m \geq n$, the computational complexity of these approaches is $O(m)$ for the proposed algorithm utilizing the selected saliency and image embedding method $O = O(m) + O(n) \approx O(m)$.

5.   CONCLUSION

This study proposed a novel blind image watermarking technique that capitalizes on robust saliency features, slightly adjusted post-watermark embedding, and a reliable learning kernel achieved through a comprehensive saliency database and robust learning method. While each of these elements has been individually explored in previous studies, this paper showcases the efficiency derived from their integration. Notably, saliency features of sub-regions are formulated and trained to facilitate embedding and extracting watermarks from the sub-regions of the host image.

The methodology exhibits promising qualities in terms of imperceptibility and watermark stability, as evidenced by experimental results on a standardized database. Its simplicity and computational efficiency make it highly suitable for promoting the utilization of saliency features. Additionally, the integration of effective saliency models offers versatile strategies for implementing blind image watermarking in various applications, particularly in the realms of authentication mechanisms and anti-forgery measures.

REFERENCES

[1] N. Ahmed, "How I came up with the discrete cosine transform," *Digital Signal Processing*, vol. 1, no. 1, pp. 4–5, 1991.

[2] A. Basu, S. Talukdar, N. Sengupta, A. Kar, S. L. Chakraborty, and S. K. Sarkar, "On the implementation of a saliency based digital watermarking," in *Information Systems Design and Intelligent Applications: Proceedings of Second International Conference INDIA 2015, Volume 1.* Springer, 2015, pp. 447–455.

[3] A. Ben-Hur, D. Horn, H. T. Siegelmann, and V. Vapnik, "Support vector clustering," *Journal of Machine Learning Research*, vol. 2, no. Dec, pp. 125–137, 2001.

[4] D. Bhowmik, M. Oakes, and C. Abhayaratne, "Visual attention-based image watermarking," *IEEE Access*, vol. 4, pp. 8002–8018, 2016.

[5] D. Brunet, E. R. Vrscay, and Z. Wang, "On the mathematical properties of the structural similarity index," *IEEE Transactions on Image Processing*, vol. 21, no. 4, pp. 1488–1499, 2011.

[6] F. Cayre, C. Fontaine, and T. Furon, "Watermarking security: theory and practice," *IEEE Transactions on Signal Processing*, vol. 53, no. 10, pp. 3976–3987, 2005.

[7] C. De Vleeschouwer, J.-F. Delaigle, and B. Macq, "Invisibility and application functionalities in perceptual watermarking an overview," *Proceedings of the IEEE*, vol. 90, no. 1, pp. 64–77, 2002.

[8] S. Fang, J. Li, Y. Tian, T. Huang, and X. Chen, "Learning discriminative subspaces on random contrasts for image saliency analysis," *IEEE Transactions on Neural Networks and Learning Systems*, vol. 28, no. 5, pp. 1095–1108, 2016.

[9] Q. Hou, M.-M. Cheng, X. Hu, A. Borji, Z. Tu, and P. H. Torr, "Deeply supervised salient object detection with short connections," in *Proceedings of The IEEE Conference on Computer Vision and Pattern Recognition*, 2017, pp. 3203–3212.

[10] X. Hou, J. Harel, and C. Koch, "Image signature: Highlighting sparse salient regions," *IEEE Transactions on Pattern Analysis and Machine Intelligence*, vol. 34, no. 1, pp. 194–201, 2011.

[11] L. Itti, C. Koch, and E. Niebur, "A model of saliency-based visual attention for rapid scene analysis," *IEEE Transactions on Pattern Analysis and Machine Intelligence*, vol. 20, no. 11, pp. 1254–1259, 1998.

[12] I. T. Jolliffe, "Principal component analysis: a beginner's guide - I. introduction and application," *Weather*, vol. 45, no. 10, pp. 375–382, 1990.

[13] J. Li, H. Zhang, J. Wang, Y. Xiao, and W. Wan, "Orientation-aware saliency guided jnd model for robust image watermarking," *IEEE Access*, vol. 7, pp. 41 261–41 272, 2019.

[14] J. Mielikainen, "Lsb matching revisited," *IEEE Signal Processing Letters*, vol. 13, no. 5, pp. 285–287, 2006.

[15] B. Pfitzmann, "Information hiding terminology," *Lecture Notes in Computer Science*, vol. 1174, pp. 347–350, 1996.

[16] N. Ponomarenko, O. Ieremeiev, V. Lukin, K. Egiazarian, and M. Carli, "Modified image visual quality metrics for contrast change and mean shift accounting," in *2011 11th International Conference The Experience of Designing and Application of CAD Systems in Microelectronics (CADSM)*. IEEE, 2011, pp. 305–311.

[17] I. E. Richardson, *H. 264 and MPEG-4 Video Compression: Video Coding for Next-Generation Multimedia*. John Wiley & Sons, 2004.

[18] N. Riche, M. Mancas, B. Gosselin, and T. Dutoit, "Rare: A new bottom-up saliency model," in *2012 19th IEEE International Conference on Image Processing*. IEEE, 2012, pp. 641–644.

[19] H. J. Seo and P. Milanfar, "Nonparametric bottom-up saliency detection by self-resemblance," in *2009 IEEE Computer Society Conference on Computer Vision and Pattern Recognition Workshops*. IEEE, 2009, pp. 45–52.

[20] L. Tian, N. Zheng, J. Xue, C. Li, and X. Wang, "An integrated visual saliency-based watermarking approach for synchronous image authentication and copyright protection," *Signal Processing: Image Communication*, vol. 26, no. 8-9, pp. 427–437, 2011.

[21] D. D. Wackerly, W. Mendenhall, and R. L. Scheaffer, *Mathematical Statistics with Applications*. Thomson Brooks/Cole Belmont, CA, 2008, vol. 7.

[22] W. E. Winkler *et al.*, "Overview of record linkage and current research directions," *Bureau of the Census*, vol. 25, no. 4, pp. 603–623, 2006.

[23] L. Wu, J. Zhang, W. Deng, and D. He, "Arnold transformation algorithm and anti-arnold transformation algorithm," in *2009 First International Conference on Information Science and Engineering*. IEEE, 2009, pp. 1164–1167.

[24] H. Xu, J. Wang, and H. J. Kim, "Near-optimal solution to pair-wise lsb matching via an immune programming strategy," *Information Sciences*, vol. 180, no. 8, pp. 1201–1217, 2010.